www.advelectronicmat.de

Versatile Contact Engineering on β -Ga₂O₃ Using EGaIn for Schottky Diodes and MESFET Applications

Gyeong Seop Kim, Jin Hyuk Choi, Min-gu Kim,* Ji-Hoon Kang,* and Young Tack Lee*

Beta gallium oxide (β -Ga₂O₃) has emerged as a promising ultrawide bandgap n-type semiconductor for large-area circuit integration and high-power device applications in the field of 5G and AI technology. However, β -Ga₂O₃ has a critical problem in Ohmic contact formation using a traditional metallization method. In this study, a low-temperature fabrication strategy is successfully demonstrated of an Ohmic contact electrode, employing eutectic gallium indium (EGaIn) liquid metal on β -Ga₂O₃ active channel material for Schottky diode circuit and metal semiconductor field effect transistor (MESFET) applications. The selective screen-printing of Ohmic and rectifying contacts enables monolithic integration of symmetric and asymmetric device architectures, including source/drain electrodes, Schottky diodes, and FETs without additional post-thermal annealing and etching processes. The β -Ga₂O₃/Au Schottky diodes exhibit good rectifying properties of a current on/off ratio of 10⁷ and an ideality factor (η) of 1.63, while the MESFET devices demonstrate a drain current on/off ratio of \approx 3.1 × 10⁶.

1. Introduction

Gallium oxide (Ga_2O_3) is well well-known polymorphism material, which has five crystalline phases of α , β , γ , δ , and

G. S. Kim, J. H. Choi, J.-H. Kang, Y. T. Lee Department of Electrical and Computer Engineering Inha University Incheon 22212, Republic of Korea

E-mail: jhkang57@inha.ac.kr; ytlee@inha.ac.kr

M.-gu Kim
Department of Medical Engineering
Yonsei University
Seoul 03722, Republic of Korea
E-mail: mgk@yonsei.ac.kr

J.-H. Kang, Y. T. Lee
Department of Electrical and Electronic Engineering
Inha University

Incheon 22212, Republic of Korea

J.-H. Kang Program in Semiconductor Convergence Inha University Incheon 22212, Republic of Korea

The ORCID identification number(s) for the author(s) of this article can be found under https://doi.org/10.1002/aelm.202500332

© 2025 The Author(s). Advanced Electronic Materials published by Wiley-VCH GmbH. This is an open access article under the terms of the Creative Commons Attribution License, which permits use, distribution and reproduction in any medium, provided the original work is properly cited.

DOI: 10.1002/aelm.202500332

 ϵ . [1-3] Among them, beta gallium oxide $(\beta$ -Ga₂O₃), an ultra-wide bandgap (UWB, 4.8 eV) semiconductor, is a very promising n-type active channel material in future electronics such as 5G and AI technologies due to its excellent electrical and optical properties.[4-8] From these reasons, many researchers focused on the β -Ga₂O₃ to achieve higher power efficiency at high voltages and high temperatures, and to reduce energy waste for zero carbon emission. However, β -Ga₂O₃ has been reported to be difficult to form proper Ohmic contact with former metal electrodes, through metal deposition and lift-off processes based on conventional thin film technology.[4,9,10] To solve this problem, plasma etching and post-thermal treatment processes are necessary to achieve good Ohmic contact properties on β -Ga₂O₃. [4,5,10–17]

Because these additional processes could create oxygen vacancies (V_O s), and the generated V_O acted as a donor (donated electron) by increasing the electron concentration at the β -Ga₂O₃ channel surface. As a result, the electron doping effect brings good Ohmic contact properties at the interface of β -Ga₂O₃ and deposited metal electrodes.

In the research field of metal oxide (MO_v) semiconductors, indium (In) and gallium (Ga) are famous elements increasing the conductivity and air stability in MO_v compounds, for example, indium gallium oxide (InGaO_x), indium-tin oxide (InSnO), and indium-gallium-zinc oxide (InGaZnO) were studied for many applications.[18-22] Furthermore, gallium-indium (GaIn) compound material, especially eutectic GaIn (EGaIn, 75 wt.% Ga, 25 wt.% In), emerging liquid metal (melting temperature of 15.5 °C), has been attracted much attention for flexible electrode in research field of smart wearable device and medical application due to its high electrical conductivity ($\sigma = 3.4 \times 10^6 \,\Omega^{-1} \text{m}^{-1}$), nontoxicity, and easy fabrication process.[23-26] Interestingly, EGaIn would be easy to form the gentle compound structure with the β-Ga₂O₃ channel by creating InGaO_x compound at the interface according to the diffusion process of In element. EGaIn could form the thin native oxide layers (thickness of \approx 3 nm) at the surface under the ambient air (oxygen) and possess high surface tension.[27-30] Therefore, the patterned EGaIn electrodes could maintain their structural stability even through a combination of conventional photolithography and the lift-off processes for micro-scaled electronic devices. [23,31,32] In this study, we demonstrate a β -Ga₂O₃-based junction device by utilizing EGaIn liquid

2199160x, 2025, 16, Downloaded from https://adanced.on.inlinibitary.wikly.com/ob/10.1002/aclm.202500332 by Yonsei University Med Library, Wiley Online Library on 114/10/2055, See the Terms and Conditions (https://onlinelibrary.wikley.com/terms-nd-conditions) on Wiley Online Library or rules of use; OA articles are governed by the applicable Centric Commons

www.advancedsciencenews.com



www.advelectronicmat.de

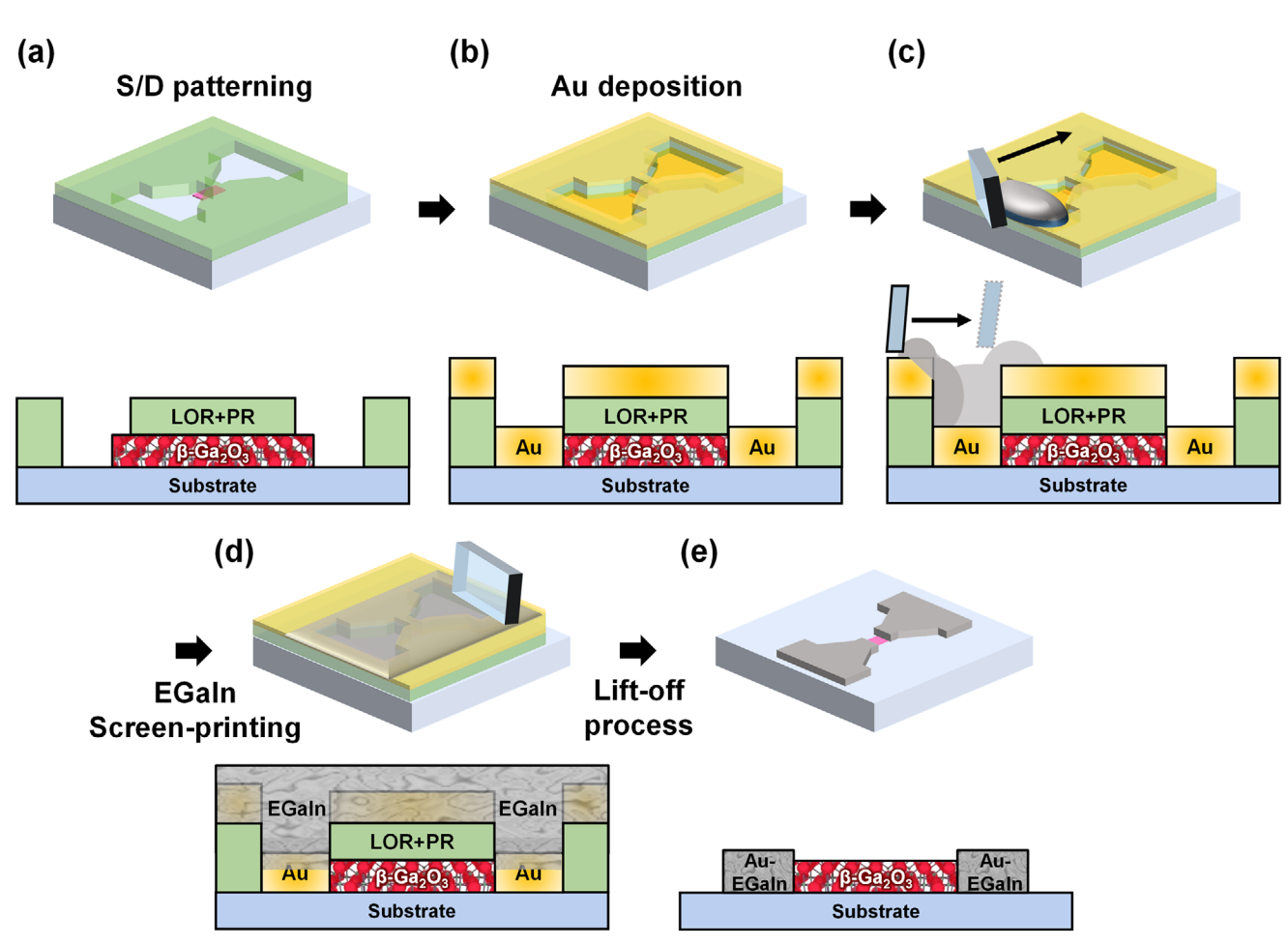


Figure 1. The schematic design (diagonal view and cross-section) fabrication processes of EGaIn S/D electrodes by using photolithography and lift-off process. a) Schematic of the after spin-coating PR and LOR. b) Schematic after Au sputtering for the buffer layer on β-Ga₂O₃. c) Schematic of fabricating EGaIn with a PDMS brush. d) The gradual diffusion of EGaIn into Au over time. e) Schematic after the lift-off process with acetone.

metal as an Ohmic contact electrode in place of conventionally deposited thin-film metal electrodes. While the flexible properties of EGaIn have been extensively investigated in prior studies, [33–39] the present work specifically examines the Ohmic contact characteristics of EGaIn with β -Ga₂O₃ semiconductor channels. Based on the diffusion phenomenon of liquid metal, the intrinsic advantages of EGaIn as an electrode material were systematically exploited to enable the development of advanced electronic devices.[27,40,41] Furthermore, the selective formation of Ohmic and non-Ohmic (rectifying) contacts on β -Ga₂O₃ semiconductor enables the fabrication of both symmetric and asymmetric device architectures, including source and drain (S/D) electrodes, metalsemiconductor (MS) Schottky diodes, and metal-semiconductor field-effect transistors (MESFET) as well. These findings underscore the potential of EGaIn liquid metal electrodes in facilitating the realization of high-performance β-Ga₂O₃-based electronic devices.

2. Results and Discussion

The single crystal monoclinic β -Ga $_2$ O $_3$ was used after being cleaved along the (010) crystal plane the largest lattice parame-

ter (or inter-distance between planes) of a[100] = 1.22 nm, b[010]= 0.304 nm, c[001] = 0.580 nm, β = 103.83°. The monoclinic Sn-doped n-type β -Ga₂O₃ crystal was prepared with an electron concentration (n) of 3.5×10^{17} cm⁻³. Figure 1 shows 3D illustrations and cross-sectional device schematics for the EGaIn S/D electrodes fabrication method by using conventional photolithography and lift-off processes. The substrate was cleaned in the order of acetone, ethanol, and isopropyl alcohol (IPA), each for 15 min in the ultrasonicator. And then, β -Ga₂O₃ flakes were mechanically exfoliated from a bulk crystal and transferred to the targeted substrate through the direct imprinting dry transfer method by using polydimethylsiloxane (PDMS) elastomer stamps. After then, the bilayer of photoresist (PR) and lift-off resist (LOR) was sequentially spin-coated, and the S/D electrode patterns were defined by UV exposure and development processes as shown in Figure 1a. As an adhesive buffer layer, a 45 nm-thick Au thin film was deposited by using a DC magnetron sputtering system at the 3D Convergence Center of Inha University (Figure 1b). Subsequently, the EGaIn liquid metal (>99.99% trace metal basis, Sigma-Aldrich) was applied and uniformly cast on the Au buffer layer by the selective screen-printing method with a PDMS brush, as shown in Figure 1c,d. The brushed EGaIn

2199160x, 2025, 16, Downloaded from https

doi/10.1002/aelm.202500332 by Yonsei University Med Library, Wiley Online Library on [14/10/2025]. See the Terms and Condition

nditions) on Wiley Online Library for rules of use; OA articles are governed by the applicable Creative Commons

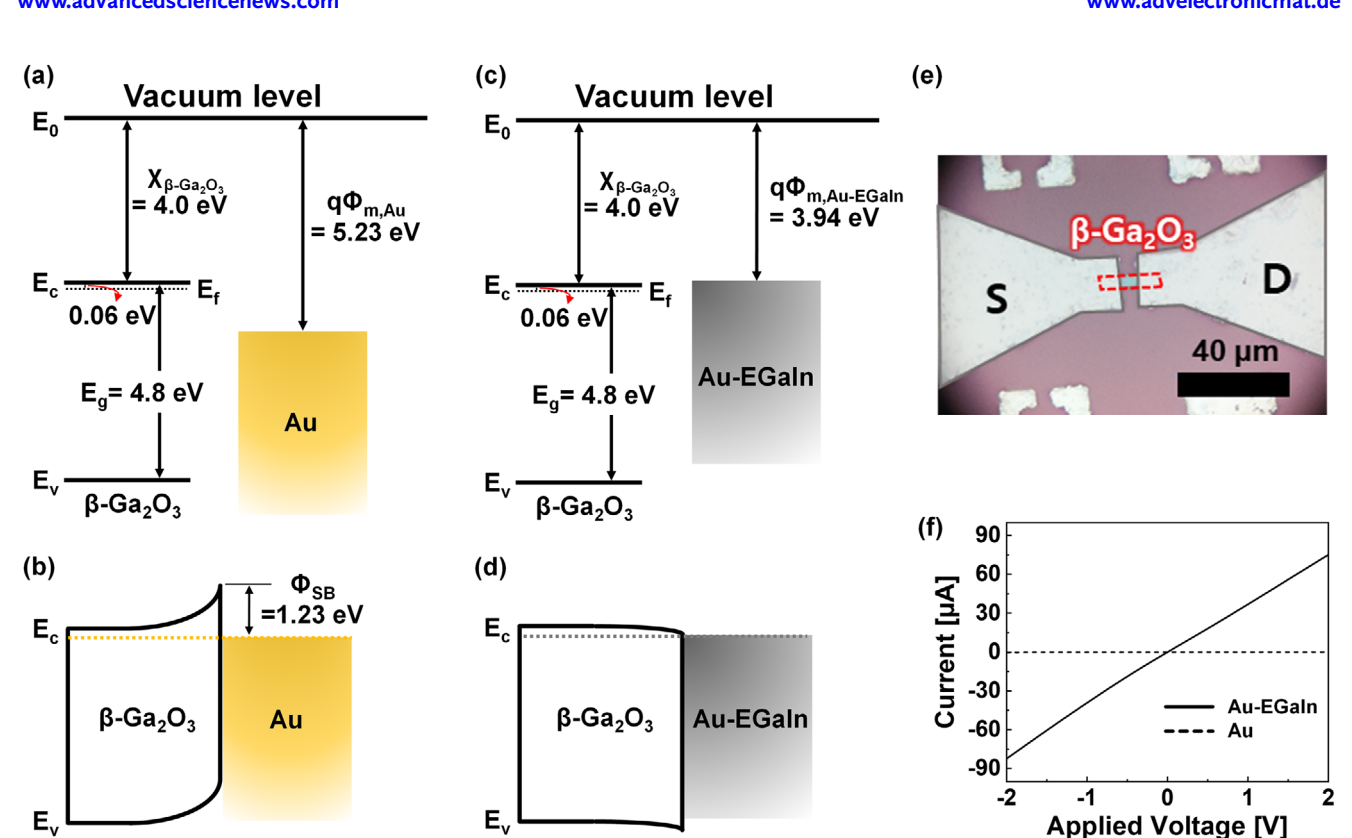


Figure 2. a) Energy Band diagram of β -Ga₂O₃, Au, Au-EGaIn (before junction). b) Energy band diagrams of β -Ga₂O₃/Au Schottky contact. c) Energy Band diagram of β -Ga₂O₃, Au-EGaIn (before junction). d) Energy band diagrams of Au-EGaIn/ β -Ga₂O₃ Ohmic contact. e) OM image and f) *I*–V characteristics curves of β -Ga₂O₃ channel-based symmetric devices of β -Ga₂O₃/Au Schottky (dashed line) and Au-EGaIn/ β -Ga₂O₃ Ohmic contact (Solid line).

gradually diffused into the Au electrodes and formed the composite of Au and EGaIn (Au-EGaIn). And finally, the patterned Au-EGaIn electrodes were successfully fabricated on the β -Ga₂O₃ channel through a lift-off process for Ohmic contact electrodes (Figure 1e).

Figure 2a,b shows energy band diagrams of *β*-Ga₂O₃/Au contact for before and after junction under thermal equilibrium state, respectively. The energy band information, such as electron affinity ($X_{\beta\text{-Ga2O3}} = 4.0 \text{ eV}$), bandgap ($E_{g, \beta\text{-Ga2O3}} = 4.8 \text{ eV}$), and electron effective mass ($m_e^* = 0.3 m_e$) of *β*-Ga₂O₃, work function of Au ($\Phi_{\text{M,Au}} = 5.23 \text{ eV}$) were referred to previous literatures.^[42,43] From the material information, we could calculate the Fermi energy level (E_F) of *β*-Ga₂O₃ to be 4.064 eV through equation (Equation (1)) as below, as well as, Schottky barrier (Φ_{SB}) of 1.23 eV from the *β*-Ga₂O₃/Au contact as depicted in Figure 1b.

$$E_F = E_i + kT ln\left(\frac{N_D}{n_i}\right) \tag{1}$$

Where, E_i is the intrinsic Fermi energy (mid-point of bandgap), N_D is the doping concentration of Sn donor ($N_D \approx n$), and we could estimate intrinsic carrier concentration (n_i) to be 1.97×10^{-22} cm⁻³ through equation (Equation (2)).

$$n_i = N_C e^{-\frac{E_C - E_i}{kT}} \tag{2}$$

 N_{C_s} which denotes the effective state density, was calculated equation (Equation (3)) to be $4.11 \times 10^{18} \text{ cm}^{-3}$.

$$N_C = 2\left(\frac{2\pi m_e^* kT}{h^2}\right)^{3/2} \tag{3}$$

On the other hand, Au-EGaIn electrode shows quite different work function ($\Phi_{M,Au-FGaIn}$) of 3.94 eV (Figure 2c), observed from UV photoelectron spectroscopy (UPS) analysis (Figure S1, Supporting Information), is smaller than $X_{\beta\text{-}Ga2O3}$, therefore, the Au-EGaIn electrodes could form good Ohmic contact with β -Ga₂O₃ semiconductor as shown in Figure 2d. Figure 2e shows an optical microscopic (OM) image of a symmetric β -Ga₂O₃ active channel device fabricated with Au-EGaIn S/D electrodes. The currentvoltage (I–V) characteristic curves, obtained from Au S/D and Au-EGaIn S/D were shown in Figure 2f at applied voltage (V_A) of -2to 2 V. The β -Ga₂O₃/Au Schottky contacts show zero current level (dashed line) while the Au-EGaIn/ β -Ga₂O₃ Ohmic contacts allow to flow high current of 82 µA at the applied voltage of 2.0 V, well obeying Ohm's law (solid line). Based on these results, we could conclude that Au-EGaIn electrodes are good candidate for forming an Ohmic contact to β -Ga₂O₃ active channel material while the single Au electrodes create Schottky contact property.

From the Au-EGaIn electrode fabrication method, we investigated symmetric (both side Ohmic contacts) and asymmetric (one side Schottky contact) global gate transistor devices fabricated on 200 nm thick SiO₂/p⁺-Si substrate, as shown in

and-conditions) on Wiley Online Library for rules of use; OA articles are governed by the applicable Creative Commons

www.advelectronicmat.de

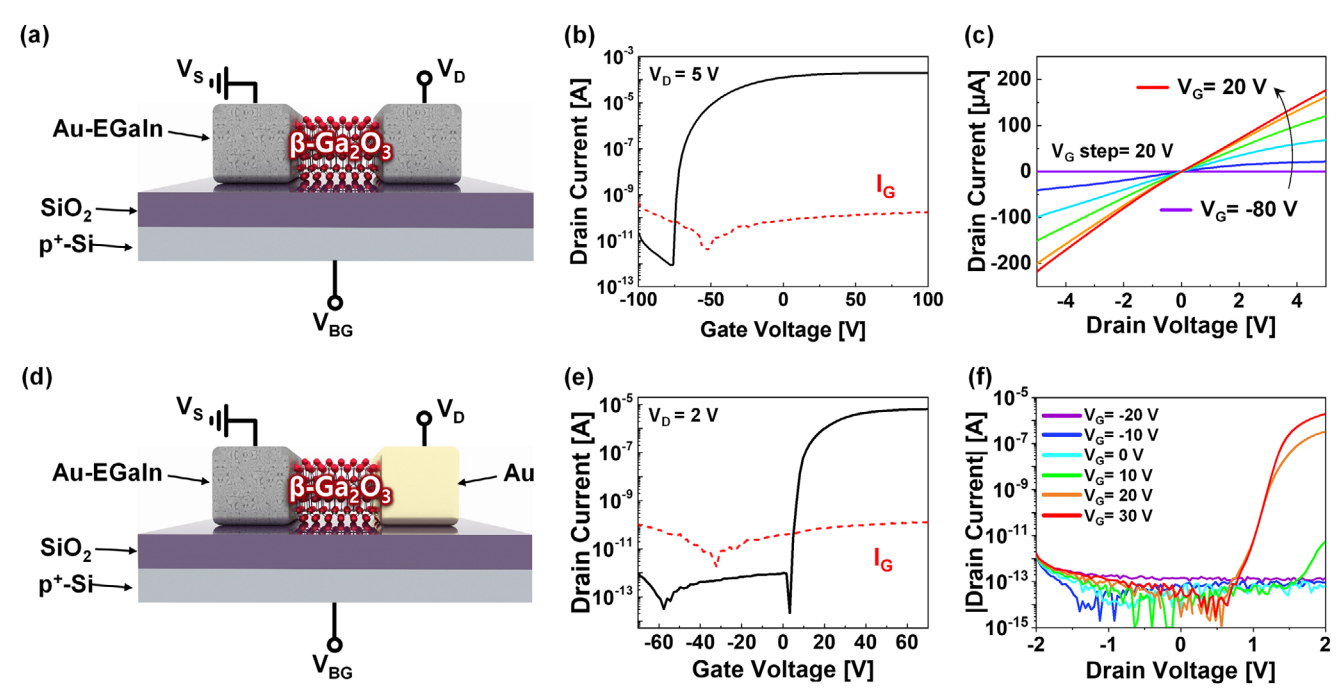


Figure 3. Device schematic views, Transfer and Output characteristics. a) 3D schematic of the symmetric device fabricated on a p^+ -Si substrate. b) Transfer characteristics of the symmetric device, where the black solid line shows the drain current and the red dashed line represents the leakage current. c) Output characteristics of the symmetric device measured with a V_G step of 20 V. d) 3D schematic of the asymmetric device fabricated on a p^+ -Si substrate. e) Transfer characteristics of the asymmetric device, with line representations consistent with those in (b). f) Output characteristics of the asymmetric device measured with a V_G step of 10 V.

Figure 3. Figure 3a,b respectively show the schematic of the symmetric device configuration and the drain current-gate voltage (I_D-V_C) transfer characteristics curve at the drain voltage (V_D) of 5 V for a bottom-gate voltage (V_{BG}) sweep range of -70 to 70 V. Figure 3c presents the drain current—drain voltage (I_D-V_D) output characteristics curves of the symmetric device, which has both Au-EGaIn S/D electrodes, where the V_D sweep range was -5 to 5 V and the varied V_{BG} –80 to 20 V with 20 V increments. These results would be clear evidence for achieving the good Ohmic properties between the Au-EGaIn and β -Ga₂O₃ active channel material. In contrast, Figure 3d,e show the schematic of the asymmetric device configuration and I_D-V_G transfer characteristics curve at V_D of 2 V for V_{BG} sweep range of -70-70 V, respectively. Figure 3f displays the gate-induced I-V rectifying characteristic curves of the asymmetric transistor device, which has one side Au-EGaIn electrode as an Ohmic source and the other side Au Schottky drain electrode for the V_D range of -2 to 2 V with the varied V_{BG} of $-20\ \text{to}\ 30\ \text{V}$ by 10 V increments. The asymmetric configuration transistor demonstrated gate-induced diode-like behavior. Although p+-Si global gate could control the carrier concentration of the β -Ga₂O₃ active channel; however, it is a disadvantage for achieving faster switching performance, owing to its RC delay from the gate capacitance. As a result, we could expect that the flat band condition of β -Ga₂O₃ active channel material has high conductivity enough to use for rectifying device-based circuit applications via electrode engineering fabricated on the glass substrate rather than p+-Si substrate. To address this issue, the β-Ga₂O₃/Au Schottky junction device has been fabricated on a glass substrate, as illustrated in Figure 4.

Figure 4a,b shows OM image and the device schematic of the β -Ga₂O₃ active channel based one side Schottky diode rectifying device fabricated on a glass substrate created with one side Au electrode, and the *I–V* characteristics curve is shown in Figure 4c for applying voltage of -2 to 2 V. The inset figure is the energy band diagram of Au-EGaIn/β-Ga₂O₃/Au system under thermal equilibrium state. The on/off current ratio and the ideality factor (η) at the β -Ga₂O₃/Au Schottky junction were estimated to $\approx 10^7$ and 1.63, respectively. The turn-on voltage was measured \approx 1.18 eV, which is very similar to the Schottky barrier height (Φ_{SB}) of 1.23 eV for Au contact, where the E_C - E_F of Sn-doped β -Ga₂O₃ is 0.06 eV, as shown in Figure 2a. Figure 4d displays the voltage transfer characteristics (VTC) curve of the half-wave rectifier circuit application consisting of the β-Ga₂O₃/Au Schottky diode and external load resistor ($R_{Load} = 680 \text{ k}\Omega$) as shown in the inset circuit diagram. As observed in Figure 4d, the input voltage (V_{in}) of 2 V was applied, the output voltage (V_{out}) was observed to be 0.68 V; however, the reduced amount of V_{out} is similar to the turn-on voltage of β -Ga₂O₃/Au Schottky diode, as shown in Figure 4c. Figure 4e is employed to present the dynamic rectification properties of the half-wave rectifying diode circuit of Figure 4d, where the input signals were square waveforms for variable frequencies of 1, 10, 100, and 500 Hz, respectively. From this result, the possible rectification process was clearly observed at the highest frequency of 500 Hz, indicating the speed limitation of the β -Ga₂O₃/Au Schottky diode.

In order to explore more advanced electronic device applications, sequentially patterned Au-EGaIn (Ohmic contact) and Au (Schottky contact) interdigital electrodes were fabricated on a single and long β -Ga₂O₃ active channel by using selective

2199160s, 2025, 16, Downloaded from https://advanced.onlinelibrary.wiley.com/doi/10.1002/aelm.202500332 by Yonsei University Med Library, Wiley Online Library on [14/10/2025]. See the Terms and Conditions (https://onlinelibrary.wiley.com/doi/10.1002/aelm.202500332 by Yonsei University Med Library, Wiley Online Library on [14/10/2025]. See the Terms and Conditions (https://onlinelibrary.wiley.com/doi/10.1002/aelm.202500332 by Yonsei University Med Library on [14/10/2025]. See the Terms and Conditions (https://onlinelibrary.wiley.com/doi/10.1002/aelm.202500332 by Yonsei University Med Library on [14/10/2025]. See the Terms and Conditions (https://onlinelibrary.wiley.com/doi/10.1002/aelm.202500332 by Yonsei University Med Library on [14/10/2025].

onditions) on Wiley Online Library for rules of use; OA articles are governed by the applicable Creative Commons

(a)

(d)

Input current [µA]

1.25

1.00 0.75

0.50

0.25

0.00 -0.25 -2

Au-EGain B-Ga20

680 kΩ

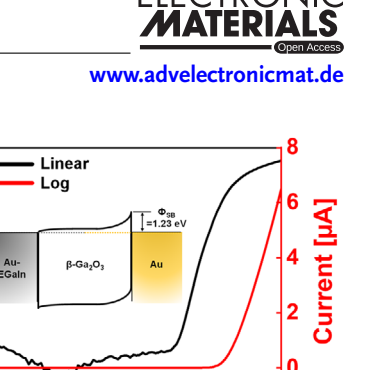
0

Input Voltage [V]

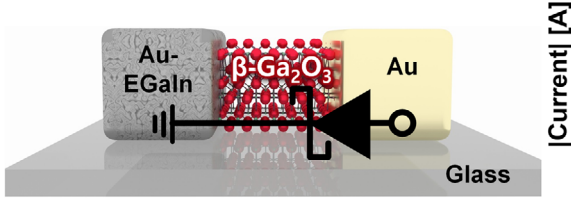
(b)

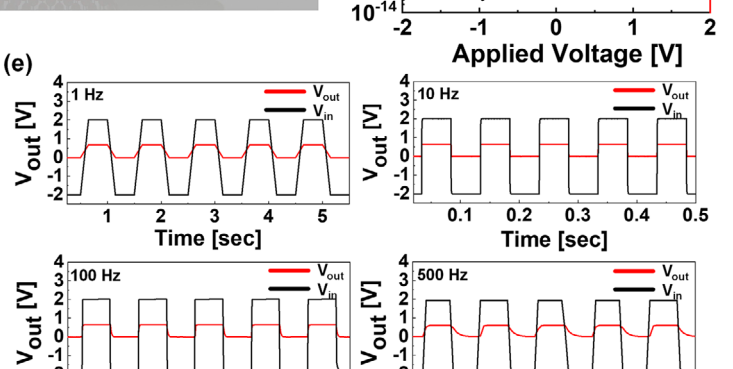
2.0

2



10





50

2

6

Time [ms]

8

10⁻⁸

10⁻¹⁰

Figure 4. a) OM image of the asymmetric diode fabricated on a glass substrate. b) 3D schematic of the asymmetric diode. c) *I–V* characteristics of the device presented in (a), with the logarithmic scale indicated by the red line and the linear scale by the black line. d) Voltage transfer characteristics of the circuit depicted in the schematic. e) Dynamic rectification performance of the circuit in (d), measured using square waves of 1, 10, 100, and 500 Hz, respectively.

10

20

30

Time [ms]

40

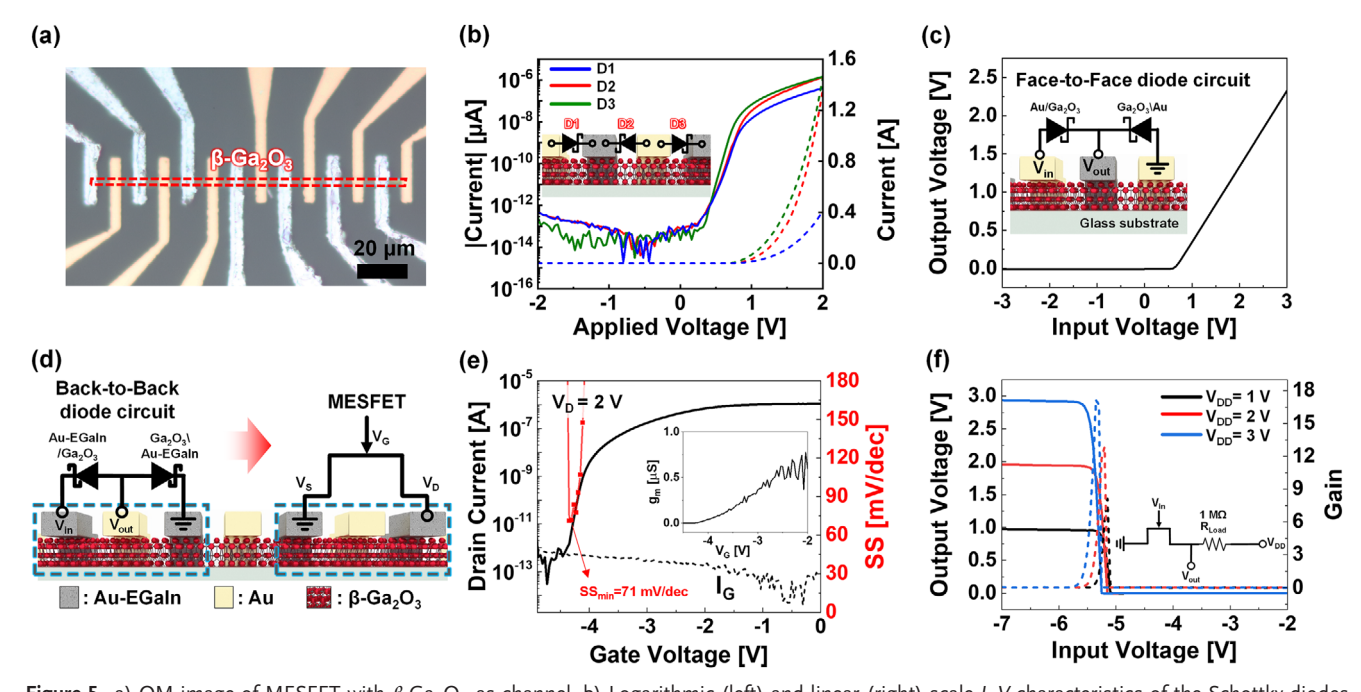


Figure 5. a) OM image of MESFET with β-Ga $_2$ O $_3$ as channel. b) Logarithmic (left) and linear (right) scale I-V characteristics of the Schottky diodes of Diodes 1, 2, and 3 within one device. c) Voltage transfer characteristics of the face-to-face diode circuit. d) Back-to-back diode circuit structure and MESFET structure. e) Transfer characteristic curve (black) and corresponding SS value (red). Inset is the transconductance (g_m) plot. f) Voltage transfer characteristics of the resistive load inverter.

ADVANCED SCIENCE NEWS

www.advancedsciencenews.com



www.advelectronicmat.de

screen-printing methods. Figure 5a shows the OM image of sequential Au-EGaIn and Au interdigital electrodes, which have several Au/β-Ga₂O₃ MS Schottky diodes. Figure 5b shows the logarithmic and linear scale I-V characteristics of three neighbor Schottky diodes (D1, D2, and D3) at the single β -Ga₂O₃ active channel among the total of 13 diodes on it. Based on this device structure, we could investigate two types of diode circuit configurations of face-to-face (F2F) and back-to-back (B2B) as shown in Figure 5c,d, respectively. In the F2F diode circuit application, the two Schottky diodes are facing each other to the common Au-EGaIn electrode. When the positive V_{in} was applied, the left diode felt the forward bias condition while the right one played as a load resistor under the effect of reverse bias, like a half-wave rectifier circuit application. Figure 5c shows the VTC curve, and the inset figure shows the circuit diagram and device scheme of the F2F diode circuit. In contrast, the B2B diode circuit would be operated in a similar way to the F2F diode system; however, the Au/β -Ga₂O₃ Schottky diodes have a large turn-on voltage, and one of the diodes remained in reverse bias, thereby preventing current flow at the low voltage. Figure S2 (Supporting Information) shows the VTC curve of the B2B diode circuit, where the turn-on voltage is determined to be ≈1.4 V. Figure 5d demonstrates the equivalent circuit of B2B diodes as a MESFET device configuration, where two Au-EGaIn electrodes are used for S/D and one Au electrode for Schottky gate electrodes. Figure 5e shows the I_D-V_G transfer characteristics curve (black line) and corresponding subthreshold swing (SS, red line) for the β-Ga₂O₃ channel-based MESFET operation. The I_D on/off ratio, threshold voltage (V_{th}), and SS minimum were extracted 3.1×10^6 , -4.1 V, and 71 mV dec⁻¹, respectively. Inset plot of Figure 5e shows the transconductance $(g_m = dI_D/dV_G)$ characteristics curve of the MESFET device. The maximum g_m was calculated to 0.77 μS at $V_G = -2.0 \text{ V}$ Figure 5f displays the VTC curve obtained from the β-Ga₂O₃ MESFET (Figure 5e) configured to a resistive-load inverter circuit application (inset). In the operation mechanisms of the resistive-load logic inverter, the low V_{in} state sets the driver MESFET as turned-off and the high $V_{\rm out}$ will come out from near the supply voltage ($V_{\mbox{\scriptsize DD}}$), whereas the zero $V_{\mbox{\scriptsize out}}$ signal generated from the turned-on state of MESFET brought by the high $V_{\rm in}$, thereby performing the inverter function. The gain values are 17, 13, and 8 for the several $V_{\rm DD}$ of 3, 2, and 1 V, respectively.

3. Conclusion

In this study, we investigated the Ohmic contact properties of β -Ga₂O₃ active channel material and gallium-based EGaIn liquid metal by utilizing the diffusion process-based selective screen-printing method for advanced electronic devices such as Schottky diode circuits and MESFET applications. Moreover, the selective screen-printing method allows damage-free and simple processing for fabricating the EGaIn electrodes onto the β -Ga₂O₃ active channel, even under low temperature, in contrast to the conventional method. β -Ga₂O₃/Au Schottky contacts show good diode performances, for example, the turn-on voltage of 1.18 eV, on/off ratio of 10⁷, and the ideality factor of 1.63, while the β -Ga₂O₃ MESFET device shows the I_D on/off ratio of 3.1 × 10⁶ and SS of 71 mV dec⁻¹. From these results, we could conclude that the EGaIn electrode is a good candidate for fabricating high-performance devices and integrated circuit applications based

on the β -Ga₂O₃ active channel. Thus, we believe that the EGaIn patterning process represents a significant key technique for β -Ga₂O₃ channel-based large area circuit and power device, as well as flexible device applications in the near future.

4. Experimental Section

Electrical Characterization: All the electrical characteristics, such as I_D - V_G transfer, I_D - V_D output, voltage transfer characteristics (VTC), and dynamic rectification properties of the half-wave rectifier were measured using a semiconductor parameter analyzer (B1500A, Keysight).

Supporting Information

Supporting Information is available from the Wiley Online Library or from the author

Acknowledgements

Y.T.L. acknowledges financial support from an INHA UNIVERSITY Research Grant

Conflict of Interest

The authors declare no conflict of interest.

Data Availability Statement

The data that support the findings of this study are available from the corresponding author upon reasonable request.

Keywords

βGa₂O₃, EGaIn, Ohmic contact, schottky diode, selective screen-printing

Received: May 16, 2025 Revised: July 31, 2025 Published online: August 26, 2025

- [1] E. A. V. Ebsworth, J. A. Connor, J. J. Turner, *Comprehensive Inorganic Chemistry*, 1st ed., Pergamon Press, Oxford, UK **1973**.
- [2] R. Roy, V. G. Hill, E. F. Osborn, J. Am. Chem. Soc. 1952, 74, 719.
- [3] H. Y. Playford, A. C. Hannon, E. R. Barney, R. I. Walton, *Chem.-A Eur. J.* 2013, 19, 2803.
- [4] H. Sheoran, V. Kumar, R. Singh, ACS Appl. Electron. Mater. 2022, 4, 2589.
- [5] S. J. Pearton, J. Yang, P. H. Cary, F. Ren, J. Kim, M. J. Tadjer, M. A. Mastro, Appl. Phys. Rev. 2018, 5, 011301.
- [6] Silvaco Inc., Atlas Simulation of a Wide Bandgap Ga₂O₃ MOSFET, Technical Report, Atlas Silvaco, Santa Clara, 2013, https://silvaco.com/ko/simulation-standard-ko/atlas-simulation-of-a-wide-bandgap-ga2o3-mosfet.
- [7] Z. Feng, X. Tian, Z. Li, Z. Hu, Y. Zhang, X. Kang, J. Ning, Y. Zhang, C. Zhang, Q. Feng, H. Zhou, J. Zhang, Y. Hao, IEEE Electron Device Lett. 2020, 41, 333.
- [8] H. H. Tippins, Phys. Rev. 1965, 140, A316.



www.advancedsciencenews.com



www.advelectronicmat.de

- [9] J. Kim, M. A. Mastro, M. J. Tadjer, J. Kim, ACS Appl. Mater. Interfaces 2017, 9, 21322.
- [10] Y. Kwon, G. Lee, S. Oh, J. Kim, S. J. Pearton, F. Ren, Appl. Phys. Lett. 2017, 110, 131901.
- [11] J. Kim, M. J. Tadjer, M. A. Mastro, J. Kim, J. Mater. Chem. C 2019, 7, 8855
- [12] K. T. Kim, H. J. Jin, W. Choi, Y. Jeong, H. G. Shin, Y. Lee, K. Kim, S. Im, Adv. Funct. Mater. 2021, 31, 2010303.
- [13] J. X. Chen, X. X. Li, H. P. Ma, W. Huang, Z.-G. Ji, C. Xia, H.-L. Lu, D. W. Zhang, ACS Appl. Mater. Interfaces 2019, 11, 32127.
- [14] H. J. Kim, S. Hong, C. Jang, H.-J. Jin, H. Woo, H. Bae, S. Im, *ACS Nano* **2024**, *18*, 8546.
- [15] H. J. Jin, H. Bae, J. T. Im, S. Im, Appl. Phys. Lett. 2024, 125, 203507.
- [16] K. T. Kim, T. Kim, Y. Jeong, S. Park, J. Kim, H. Cho, S.-K. Cha, Y.-S. Kim, H. Bae, Y. Yi, S. Im, ACS Nano 2023, 17, 3666.
- [17] J. Kim, J. Kim, ACS Appl. Mater. Interfaces 2020, 12, 7310.
- [18] J. Feldl, M. Feneberg, A. Papadogianni, J. Lähnemann, T. Nagata, O. Bierwagen, R. Goldhahn, M. Ramsteiner, Appl. Phys. Lett. 2021, 119, 042101.
- [19] J.-I. Park, J. H. Heo, S.-H. Park, K. I. Hong, H. G. Jeong, S. H. Im, H.-K. Kim, J. Power Sources 2017, 341, 340.
- [20] M. Zhao, Z. Zhang, Y. Xu, D. Xu, J. Zhang, Z. Huang, Phys. Status Solidi A 2020, 217, 1900773.
- [21] H. Chen, Y. Cao, J. Zhang, C. Zhou, Nat. Commun. 2014, 5, 4097.
- [22] F. Mo, Y. Tagawa, C. Jin, M. Ahn, T. Saraya, T. Hiramoto, M. Kobayashi, *IEEE J. Electron Devices Soc.* **2020**, *8*, 717.
- [23] M. D. Dickey, R. C. Chiechi, R. J. Larsen, E. A. Weiss, D. A. Weitz, G. M. Whitesides, Adv. Funct. Mater. 2008, 18, 1097.
- [24] J. Dong, Y. Zhu, Z. Liu, M. Wang, Nanomaterials 2021, 11, 3400.
- [25] S. H. Jeong, K. Hjort, Z. Wu, Sci. Rep. 2015, 5, 8419.
- [26] J. G. Aguila, In Situ SEM Solidification Study of Ga and eGaIn: A Characterization Technique for Monitoring the Microstructural Evolution of Liquid Metals, Technical Report, California Polytechnic State University, San Luis Obispo 2018.
- [27] G. Lu, E. Ni, Y. Jiang, W. Wu, H. Li, Small 2024, 20, 2304147.

- [28] S. A. Agnew, A. P. Tiwari, S. W. Ong, M. S. Rahman, W. J. Scheideler, Small 2024, 20, 2403801.
- [29] R. C. Chiechi, E. A. Weiss, M. D. Dickey, G. M. Whitesides, Angew. Chem., Int. Ed. 2008, 47, 142.
- [30] K. Doudrick, S. Liu, E. M. Mutunga, K. L. Klein, V. Damle, K. K. Varanasi, K. Rykaczewski, Langmuir 2014, 30, 6867.
- [31] M. Kim, D. K. Brown, O. Brand, Nat. Commun. 2020, 11, 1002.
- [32] Y. C. Sun, G. Boero, J. Brugger, ACS Appl. Electron. Mater. 2021, 3, 5423.
- [33] S. Kim, B. Yoo, M. Miller, D. Bowen, D. J. Pines, K. M. Daniels, Sens. Actuators, A 2022, 342, 113659.
- [34] S. D. Hossain, A. Arif, B. Lohani, R. C. Roberts, Flexible EGaIn Liquid Metal Microstrip Patch Antenna Based Pressure Sensor, IEEE, Sydney, Australia 2021.
- [35] J. Yang, J. Cao, J. Han, Y. Xiong, L. Luo, X. Dan, Y. Yang, L. Li, J. Sun, Q. Sun, Nano Energy 2022, 101, 107582.
- [36] C. Wei, H. Fei, Y. Tian, Y. An, G. Zeng, J. Feng, Y. Qian, Small 2019, 15, 1903214.
- [37] J. Gao, J. Ye, S. Chen, J. Gong, Q. Wang, J. Liu, ACS Appl. Mater. Interfaces 2021, 13, 17093.
- [38] G. H. Lee, Y. R. Lee, H. Kim, D. A. Kwon, H. Kim, C. Yang, S. Q. Choi, S. Park, J.-W. Jeong, S. Park, Nat. Commun. 2022, 13, 2643.
- [39] W. Liu, J. Sun, W. Qiu, Y. Chen, Y. Huang, J. Wang, J. Yang, Nanoscale 2019. 11. 21740.
- [40] Z. Xing, G. Zhang, J. Ye, Z. Zhou, J. Gao, B. Du, K. Yue, Q. Wang, J. Liu, Adv. Mater. 2023, 35, 2209392.
- [41] Y. Chi, P. V. Kumar, J. Zheng, C. Kong, R. Yu, L. Johnston, M B. Ghasemian, Md. A Rahim, T. Kumeria, D. Chu, X. Lu, G. Mao, K. Kalantar-Zadeh, J. Tang, ACS Nano 2023, 17, 17070.
- [42] M. Higashiwaki, A. Kuramata, H. Murakami, Y. Kumagai, J. Phys. D: Appl. Phys. 2017, 50, 333002.
- [43] A. Mock, R. Korlacki, C. Briley, V. Darakchieva, B. Monemar, Y. Kumagai, K. Goto, M. Higashiwaki, M. Schubert, *Phys. Rev. B* 2017, 96, 245205.